Int J Theor Phys (2011) 50:2134–2143
DOI 10.1007/s10773-010-0635-4

The Massless Dirac Equation in the Refrigerator

José M. Cerveró · Enrique Díez

Received: 22 September 2010 / Accepted: 9 December 2010 / Published online: 29 December 2010

Abstract We discuss the physics of graphene, which has recently generated great excitement in both the experimental and the theoretical realms. From the theoretical side, the main novelty is that 2D-graphene obeys massless Dirac instead of massive Schrödinger equations. The Dirac equation has mainly been used for the description of the high-energy relativistic physics of electrons and photons. However, here we shall be dealing with electron transport at much lower energy and hence temperature. We also discuss the so-called Klein paradox that can actually be seen, doing away with its paradoxical status forever. The Quantum Hall Effect in graphene also exhibits surprising features related to the Dirac sea.

Keywords Dirac equation · Klein paradox and QHE · Experimental graphene

1 Introduction

Graphene is a strictly two-dimensional slab of carbon with a honeycomb geometric structure. The electronic structure of graphene follows from a simple nearest- neighbor, tight-binding approximation. Graphene has two atoms per unit cell, which results in two conical points per Brillouin zone where band crossing occurs. Near these crossing points, the electron energy is linearly dependent on the wave vector. Actually, this behavior follows from symmetry considerations, and is therefore robust with respect to long-range hopping processes. Amazingly enough, all these facts were already known to the scientific community in 1947 [1], but then the seeming unfeasibility of obtaining two-dimensional samples made up of just one hexagonally crystallized carbon atom slab left all these properties as a mere physical curiosity. Now that we have the technology to construct such samples,

J.M. Cerveró (✉) · E. Díez
Laboratorio de Bajas Temperaturas, Departamento de Física Fundamental, Universidad de Salamanca, 37008 Salamanca, Spain
e-mail: cervero@usal.es

E. Díez
e-mail: enrisa@usal.es

a wealth of papers has appeared in theoretical [2], experimental [3–6] and even in large reviews dealing with all aspects of the system [7].

What makes graphene so attractive for theoretical research is that its spectrum closely resembles the Dirac spectrum for massless fermions. The Dirac equation describes relativistic quantum particles with spin $\frac{1}{2}$, such as electrons. The essential feature of the Dirac spectrum, following from the basic principles of quantum mechanics and relativity theory, is the existence of antiparticles. More specifically, states at positive and negative energies (electrons and holes) are intimately linked, being described by different components of the same spinor wave function. This fundamental property of the Dirac equation is often referred to as the charge-conjugation symmetry. For Dirac particles with mass m, there is a gap between the minimal electron energy, $E_o = mc^2$, and the maximal hole energy. When the electron energy $E \gg E_o$, the energy is linearly dependent on the wavevector $k \to E = c\hbar k$. For massless Dirac fermions, the gap is zero and this linear dispersion law holds at any energy. In this case, there is an intimate relationship between the spin and motion of the particle: spin can only be directed along the propagation direction for particles or only opposite to it for antiparticles. In contrast, massive spin-$\frac{1}{2}$ particles can have two values of spin projected onto any axis. In a sense, we have a unique situation here: charged massless particles. Although this is a popular textbook example, no such particles have been observed before.

The fact that the charge carriers in graphene are described by a Dirac-like spectrum, rather than the usual Schrödinger equation for nonrelativistic quantum particles, can be seen as being a consequence of the crystal structure of graphene. This consists of two equivalent carbon sublattices. Quantum-mechanical hopping between the sublattices leads to the formation of two energy bands, and their intersection near the edges of the Brillouin zone yields the conical energy spectrum [6]. As a result, quasiparticles in graphene exhibit a linear dispersion relation $E = c\hbar k_F$, as if they were massless relativistic particles such as, for example, photons, but here the role of the speed of light is played by the Fermi velocity of value of the order: $v_F \simeq \frac{c}{300}$. Because of the linear spectrum, one can expect quasiparticles in graphene to behave differently from those in conventional metals and semiconductors, where the energy spectrum can be approximated by a parabolic dispersion relation.

In this paper we shall be dealing with the theoretical aspects of the Klein phenomenon specifically applied to graphene, with special emphasis on the problem of the transparency of a potential barrier, which is not often discussed in the literature. In the last section we shall concentrate on the anomalous Quantum Hall effect in graphene and some novel results that have recently been obtained at our laboratory.

2 The Klein Paradox Revisited. The Potential Step

The literature offers excellent reviews on the Klein paradox [8]. Here we shall be using the four dimensional formalism with a non-vanishing mass m that can gradually be set at zero. Also, the spinors propagate only in the spatial direction x_3. On the left hand side of the origin there is no potential. On the right hand side, a constant potential step V_0 is present. The solutions of spin up and down for the three-component momentum $\{p_+, p_-, p_3\}$ take the form:

$$u_\uparrow = \begin{pmatrix} 1 \\ 0 \\ \frac{cp_3}{(\mathbf{E}+mc^2)} \\ \frac{cp_+}{(\mathbf{E}+mc^2)} \end{pmatrix}; \qquad u_\downarrow = \begin{pmatrix} 0 \\ 1 \\ \frac{cp_-}{(\mathbf{E}+mc^2)} \\ \frac{-cp_3}{(\mathbf{E}+mc^2)} \end{pmatrix} \tag{1}$$

However, in our case $p_+ = p_- = 0$ and we shall simply use $p_3 \to \hbar k^-$ to refer to the one-dimensional momentum on the left hand side with *no potential* and $p_3 \to \hbar k^+$ to refer to the one-dimensional momentum on the right hand side region with a *step potential*. The incident, reflected, and transmitted waves are:

$$\psi_{inc} = \exp\{ik^- x_3\} \begin{pmatrix} 1 \\ 0 \\ \frac{c\hbar k^-}{(\mathbf{E}+mc^2)} \\ 0 \end{pmatrix} \tag{2}$$

$$\psi_{ref} = A\exp\{-ik^- x_3\} \begin{pmatrix} 1 \\ 0 \\ \frac{-c\hbar k^-}{(\mathbf{E}+mc^2)} \\ 0 \end{pmatrix} + B\exp\{-ik^- x_3\} \begin{pmatrix} 0 \\ 1 \\ 0 \\ \frac{c\hbar k^-}{(\mathbf{E}+mc^2)} \end{pmatrix} \tag{3}$$

$$\psi_{trans} = C\exp\{ik^+ x_3\} \begin{pmatrix} 1 \\ 0 \\ \frac{c\hbar k^+}{(\mathbf{E}-V_0+mc^2)} \\ 0 \end{pmatrix} + D\exp\{ik^+ x_3\} \begin{pmatrix} 0 \\ 1 \\ 0 \\ \frac{-c\hbar k^+}{(\mathbf{E}-V_0+mc^2)} \end{pmatrix} \tag{4}$$

The energy is an invariant because there is no absorption; i.e. only reflected and transmitted waves exist. Also, $B = D = 0$ because a scalar potential cannot produce spin flips. The conditions at the boundary will be discussed in two separate cases:

2.1 Case I. $V_0 < \mathbf{E} + mc^2$

The energy conservation here reads:

$$\sqrt{\left[\hbar^2 c^2 (k^-)^2 + m^2 c^4\right]} = \mathbf{E} = \sqrt{\left[\hbar^2 c^2 (k^+)^2 + m^2 c^4\right]} + V_0 \tag{5}$$

Thus, we have:

$$\begin{aligned} 1 + A &= C \\ 1 - A &= \frac{k^+}{k^-}\left\{\frac{\mathbf{E}+mc^2}{\mathbf{E}-V_0+mc^2}\right\}C \end{aligned} \tag{6}$$

Substituting in the above expression the quantities k^+ and k^-, one has:

$$1 - A = \sqrt{\frac{(\mathbf{E}-V_0-mc^2)(\mathbf{E}+mc^2)}{(\mathbf{E}-V_0+mc^2)(\mathbf{E}-mc^2)}}C = \Omega C \tag{7}$$

and solving for the constants, we obtain:

$$A = \frac{1-\Omega}{1+\Omega}; \qquad C = \frac{2}{1+\Omega} \tag{8}$$

The probability currents, j_{inc}, j_{ref} and j_{trans}, are easily calculated since the only spatial component points in the x_3 positive direction. Thus, $j = \psi^\dagger \alpha^3 \psi$, and using the correspondent spinors in each region we obtain:

$$j_{inc} = c\psi_{inc}^\dagger \alpha^3 \psi_{inc} = \frac{2c^2\hbar k^-}{\mathbf{E}+mc^2} \tag{9}$$

$$j_{ref} = c\psi^{\dagger}_{ref}\alpha^3\psi_{ref} = -A^2\frac{2c^2\hbar k^-}{\mathbf{E}+mc^2} \tag{10}$$

$$j_{trans} = c\psi^{\dagger}_{trans}\alpha^3\psi_{trans} = C^2\frac{2c^2\hbar k^+}{\mathbf{E}-V_0+mc^2} \tag{11}$$

The probability current is always conserved since there is no absorption:

$$j_{inc} + j_{ref} = j_{trans} \tag{12}$$

Finally, as one can easily check, in this case we always have $\Omega < 1$. Therefore, one can define reflexion and transmission coefficients in the usual manner as:

$$\begin{aligned}\mathcal{R} &= \left|\frac{j_{ref}}{j_{inc}}\right| = \frac{(1-\Omega)^2}{(1+\Omega)^2}\\ \mathcal{T} &= \left|\frac{j_{trans}}{j_{inc}}\right| = \frac{4\Omega}{(1+\Omega)^2}\end{aligned} \tag{13}$$

2.2 Case II. $V_0 > \mathbf{E} + mc^2$

The energy conservation here takes the form:

$$\sqrt{\left[\hbar^2c^2(k^-)^2 + m^2c^4\right]} = \mathbf{E} = V_0 - \sqrt{\left[\hbar^2c^2(k^+)^2 + m^2c^4\right]} \tag{14}$$

The conditions on the coefficients now take the form:

$$1 + A = C \tag{15}$$

$$1 - A = -\frac{k^+}{k^-}\left\{\frac{\mathbf{E}+mc^2}{V_0-\mathbf{E}-mc^2}\right\}C \tag{16}$$

Substituting in the above expression the quantities k^+ and k^-, one has:

$$1 - A = -\sqrt{\frac{(V_0-\mathbf{E}+mc^2)(\mathbf{E}+mc^2)}{(V_0-\mathbf{E}-mc^2)(\mathbf{E}-mc^2)}}C = -\Omega C \tag{17}$$

The solution is:

$$A = \frac{1+\Omega}{1-\Omega}; \qquad C = \frac{2}{1-\Omega} \tag{18}$$

The probability currents j_{inc}, j_{ref} and j_{trans} now take the form:

$$j_{inc} = c\psi^{\dagger}_{inc}\alpha^3\psi_{inc} = \frac{2c^2\hbar k^-}{\mathbf{E}+mc^2} \tag{19}$$

$$j_{ref} = c\psi^{\dagger}_{ref}\alpha^3\psi_{ref} = -A^2\frac{2c^2\hbar k^-}{\mathbf{E}+mc^2} \tag{20}$$

$$j_{trans} = c\psi^{\dagger}_{trans}\alpha^3\psi_{trans} = -C^2\frac{2c^2\hbar k^+}{V_0-\mathbf{E}-mc^2} \tag{21}$$

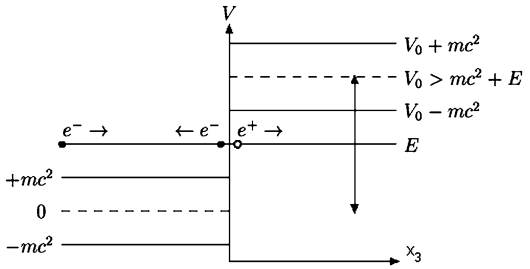

Fig. 1 The potential step when $V_0 > \mathbf{E} + mc^2$. The Dirac sea is then directly exposed to the creation of positively charged holes by the scattering of incoming negative electrons

Note, however, that the probability current is also conserved in this case since there is no absorption either. Thus, the following equation still holds:

$$j_{inc} + j_{ref} = j_{trans} \tag{22}$$

However, the reflexion and transmission coefficients cannot be defined in the usual way as they would give rise to noticeable anomalies. For large potentials compared to the total energy of the system, the momentum k^+ is real and the reflected wave rapidly oscillates in the transmission zone instead of the rapid decay expected. This is the so-called *Zitterbewegung* and it can be seen as a consequence of the appearance of a large number of solutions of negative energy when the energy of the potential step is large compared to mc^2.

On the other hand, one easily notes that in this case $\Omega > 1$, and as a result one has $|j_{ref}| > |j_{inc}|$. This result shows that the transmitted flux is in the left region, which is clearly counterintuitive. To cope with this seeming paradox, we have to define the so called *Dirac sea*. This is full of negative-energy electrons so that the total charge will be zero. It is also excitable. Electrons with positive energy can be created if one provides enough kinetic energy. In principle, the inverse process could be possible, but to prevent it we assume that all electronic states with negative energy such that $\mathbf{E} < -mc^2$ are filled with electrons. Therefore, in the case $V_0 > \mathbf{E} + mc^2$ the potential increases the energy of the electrons in the right hand side region in such a way that there exists an overlapping among the *negative continuum in the x_3^+ region* and the *positive continuum in the x_3^- region*. See Fig. 1.

In this way the electrons hitting the barrier from the left can extract additional electrons from the vacuum of the right region, which is measured as a flux of holes flowing from left to right, within the region where the potential is situated. It is now possible to understand the sign of j_{trans} by assuming that the excess of incoming electrons coming from the left region appear from the negative continuum of the Dirac sea as states that are first excited to holes from left to right and then reinterpreted as electrons from right to left. Thus, $|j_{ref}| > |j_{inc}|$, as we pointed out at the beginning of the paragraph.

To summarize. The paradox is explained as a conversion of electron-hole pairs as a result of the large value of the potential $V_0 > \mathbf{E} + mc^2$. If the mass of the "electrons" is zero this phenomenon takes place for any energy and any value of the potential. This is the case of graphene.

3 The Klein Paradox Revisited. The Potential Barrier

Let us now deal with the less known case of a potential barrier of positive magnitude V_0 and width a placed between $x_3 = 0$ and $x_3 = +a$. The reason why the barrier has not been analyzed very often within the framework of the Klein phenomenon [9] can be attributed to the

fact that the Dirac equation has always been used as a description of high-energy particles, where barriers are of almost no interest except for very few exotic cases [10]. However, in the case of graphene we are at very low temperature compared to the high-energy regime, and the samples contain barriers, as do transistors and other nanotechnological devices. Therefore, barriers play not only a role but are of paramount importance in dealing with the properties of graphene. The three spatial regions can now be written as before:

$$\psi_{inc+ref} = \exp\{ikx_3\}\begin{pmatrix} 1 \\ 0 \\ \frac{c\hbar k}{(\mathbf{E}+mc^2)} \\ 0 \end{pmatrix} + R\exp\{-ikx_3\}\begin{pmatrix} 1 \\ 0 \\ \frac{-c\hbar k}{(\mathbf{E}+mc^2)} \\ 0 \end{pmatrix} \tag{23}$$

$$\psi_{internal} = C\exp\{ik_0x_3\}\begin{pmatrix} 1 \\ 0 \\ \frac{c\hbar k_0}{(\mathbf{E}-V_0+mc^2)} \\ 0 \end{pmatrix} + D\exp\{-ik_0x_3\}\begin{pmatrix} 1 \\ 0 \\ \frac{-c\hbar k_0}{(\mathbf{E}-V_0+mc^2)} \\ 0 \end{pmatrix} \tag{24}$$

$$\psi_{transmitted} = S\exp\{ikx_3\}\begin{pmatrix} 1 \\ 0 \\ \frac{c\hbar k}{(\mathbf{E}+mc^2)} \\ 0 \end{pmatrix} \tag{25}$$

where the moments in each region take the form:

$$k_0 = \frac{1}{\hbar c}\sqrt{(\mathbf{E}-V_0+mc^2)(\mathbf{E}-V_0-mc^2)} \tag{26}$$

$$k = \frac{1}{\hbar c}\sqrt{(\mathbf{E}+mc^2)(\mathbf{E}-mc^2)} \tag{27}$$

The compatibility conditions at the frontiers are:

$$1 + R = C + D \tag{28}$$

$$1 - R = \Omega(C - D) \tag{29}$$

$$C\exp\{ik_0a\} + D\exp\{-ik_0a\} = \Omega(C\exp\{ik_0a\} - D\exp\{-ik_0a\}) = S\exp\{ika\} \tag{30}$$

where Ω has been defined as:

$$\Omega = \sqrt{\frac{(\mathbf{E}-V_0-mc^2)(\mathbf{E}+mc^2)}{(\mathbf{E}-V_0+mc^2)(\mathbf{E}-mc^2)}} \tag{31}$$

Do we also have to distinguish here between the cases $V_0 < \mathbf{E} + mc^2$ and $V_0 > \mathbf{E} + mc^2$? The answer is no, owing to the left-right symmetry of the problem. Therefore, both cases can be treated simultaneously. Solving for C and D we obtain:

$$C = \frac{2(1+\Omega)\exp\{-ik_0a\}}{(1+\Omega)^2\exp\{-ik_0a\} - (1-\Omega)^2\exp\{ik_0a\}} \tag{32}$$

$$D = \frac{-2(1-\Omega)\exp\{ik_0a\}}{(1+\Omega)^2\exp\{-ik_0a\} - (1-\Omega)^2\exp\{ik_0a\}} \tag{33}$$

Finally, we can obtain the reflexion and transmission amplitudes:

$$R = \frac{(1-\Omega^2)\sin\{k_0 a\}}{(1+\Omega^2)\sin\{k_0 a\} + 2i\Omega\cos\{k_0 a\}}$$
$$S = \frac{2i\Omega\exp\{-ika\}}{(1+\Omega^2)\sin\{k_0 a\} + 2i\Omega\cos\{k_0 a\}} \tag{34}$$

and also the reflexion and transmission coefficients:

$$\mathcal{R} = |R|^2 = \frac{\sin^2\mathbf{\Theta}\sin^2\{k_0 a\}}{\cos^2\mathbf{\Theta} + \sin^2\mathbf{\Theta}\sin^2\{k_0 a\}} \tag{35}$$

$$\mathcal{T} = |S|^2 = \frac{\cos^2\mathbf{\Theta}}{\cos^2\mathbf{\Theta} + \sin^2\mathbf{\Theta}\sin^2\{k_0 a\}} \tag{36}$$

where we have defined:

$$\sin\mathbf{\Theta} = \frac{(1-\Omega^2)}{(1+\Omega^2)} \tag{37}$$

$$\cos\mathbf{\Theta} = \frac{2\Omega}{(1+\Omega^2)} \tag{38}$$

In the case analyzed here we always have:

$$\mathcal{R} + \mathcal{T} = 1 \tag{39}$$

regardless of the value of Ω. This result seems to differ sharply from the potential step analyzed previously. However, we shall see below that there also exist various anomalous behaviours consistent with the Klein effect.

• *Zitterbewegung in the barrier*. The term $\sin^2\{k_0 a\}$ is a crucial ingredient of the oscillating behaviour in this system. Since the reflection and transmission coefficients depend critically upon this term, which in turn depends on the k_0 momentum and hence on the energy, there will be values of the momentum k_0 for which $\sin^2\{k_0 a\} = 0$, giving rise to transparency effects. Note that the oscillating function is the same as the one that, for large values of V_0, is responsible for the large oscillations of the solutions of the Dirac equation that we already know as the *Zitterbewegung*. Another surprising feature is the fact that for large values of V_0, we have $\mathcal{R} = 0$ and $\mathcal{T} = 1$. Therefore, the transmission coefficient increases rapidly towards unity and oscillates close to this value for larger energies. In other words, transmission is maximal for V_0 approaching ∞. This is in sharp contrast with non-relativistic quantum mechanics, which in this case yields $\mathcal{T} = 0$.

This behaviour can again be explained with the help of the Dirac sea. A very large value of the barrier height leaves the Dirac sea exposed to the creation of a large number of electron-hole pairs and the number of electrons to the right greatly exceeds that of the electrons at the left, making the transmission much more likely than the reflection. It should also be noted that for very small mass m the quantity Ω is close to unity, such that transparency in graphene will take place almost at zero energy.

• Finally the quantum particles in the plane behave as if the incoming electrons were hitting the barrier from any direction of the $\{x_1, x_2\}$-plane towards the barrier. Thus, the

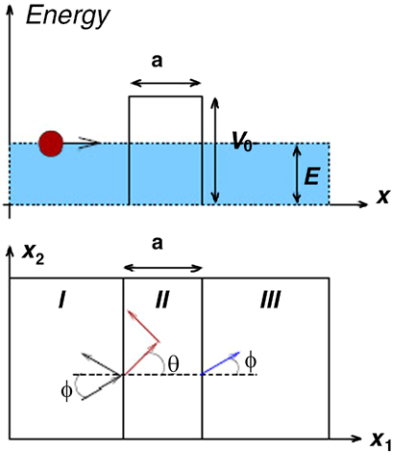

Fig. 2 (**a**) Barrier in one dimension. (**b**) Band of potential in the $\{x_1, x_2\}$-plane and incident angle of the incoming electrons $\boldsymbol{\Phi}$, where $\boldsymbol{\theta}$ is the refraction index due to the x_2 momentum component. See expressions prior to formula (3) in [10]

only additional degree of freedom is the angle $\boldsymbol{\Phi}$ between the incoming propagation and the straight line perpendicular to the barrier band. One can easily see this in Fig. 2 where (a) represents the one-dimensional case described above while (b) depicts the aerial view over the $\{x_1, x_2\}$-plane and the angle $\boldsymbol{\Phi}$. A similar calculation yields the expression for $\mathcal{R}$ and $\mathcal{T}$ as follows [10]:

$$\mathcal{R} = |R|^2 = \frac{(\sin\boldsymbol{\theta} - \sin\boldsymbol{\Phi})^2 \sin^2\{k_0 a\}}{\cos^2\boldsymbol{\theta}\cos^2\boldsymbol{\Phi} + (\sin\boldsymbol{\theta} - \sin\boldsymbol{\Phi})^2 \sin^2\{k_0 a\}} \tag{40}$$

$$\mathcal{T} = |S|^2 = \frac{\cos^2\boldsymbol{\theta}\cos^2\boldsymbol{\Phi}}{\cos^2\boldsymbol{\theta}\cos^2\boldsymbol{\Phi} + (\sin\boldsymbol{\theta} - \sin\boldsymbol{\Phi})^2 \sin^2\{k_0 a\}} \tag{41}$$

Note, however, that when $\boldsymbol{\Phi} = 0$ the system reduces to the one-dimensional case, as it should be. Finally, $\sin\boldsymbol{\theta} \neq \sin\boldsymbol{\Phi}$ since otherwise $V_0 = 0$.

4 Experimental Results: The Quantum Hall Effect and Klein Tunneling

As we have shown in the previous sections, electron transport across a barrier in graphene would allows us to construct solid-state devices in which Klein tunneling really occurs. Probably the simplest way to create a barrier in graphene is through a local top gate. Moreover, the types of carriers (electron-like or hole-like) and their density can be controlled by using the electric-field effect, rendering conventional semiconductor doping via ion implantation unnecessary. Thus, this doping via local gates [11] would allow graphene-based bipolar technology devices with junctions between hole-like and electron-like regions to be reconfigurable by using only gate voltages to distinguish p (hole-like) from n (electron-like) within a single sheet as in conventional p–n junctions.

We report the occurrence of local top gating in a single-layer graphene device that, combined with global back gating, allows individual control of different types of carriers and densities in adjacent regions of a single atomic layer. We used monolayer graphene flakes obtained by peeling graphite onto a highly doped Si wafer with a 300 nm SiO_2 top layer. They were processed in the CT-ISOM (Madrid) clean-room facilities, depositing 50/500 Angstrom Ti/Au contacts in different geometries by using e-beam nanolithography. In order

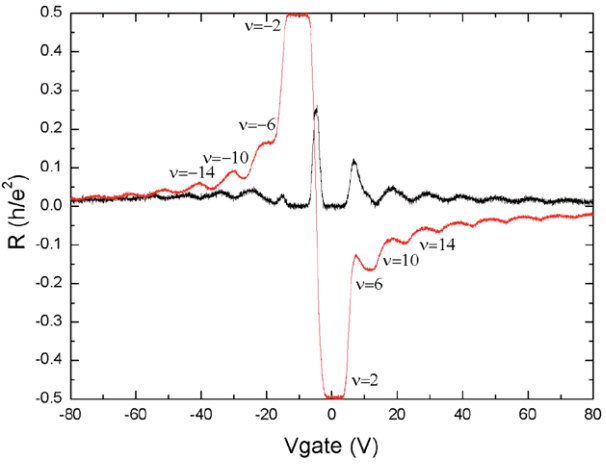

Fig. 3 Longitudinal R_{xx} (*black*) and Hall R_{xy} (*red*) resistances as a function of the gate voltage at $B_o = 8$ Tesla and 4.2 K. Several Hall plateaus are clearly resolved, in agreement with the graphene shifted sequence

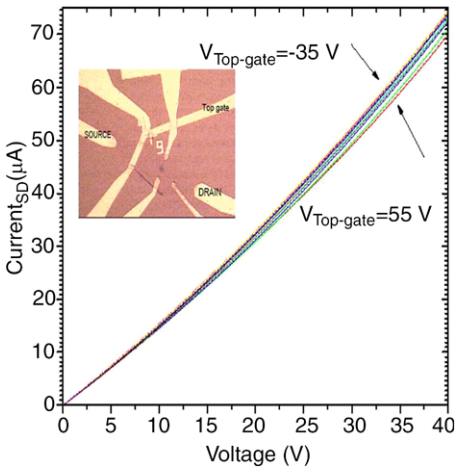

Fig. 4 Plot of source-drain current as a function of the source-drain voltage applying different top-gate voltages. The output current remains almost unmodified even for a variation of the top gate range of nearly 80 V

to form the top gate stack, we covered the whole wafer with 30 nm of SiO_2 and then grew a contact of Ti/Au with widths ranging from 200 to 800 nm.

In graphene, the conventional integer quantum Hall (QH) quantization for the conductivity, σ_{xy}, is shifted by a half-integer due to the half-filling of the $n = 0$ Landau level. The Landau levels and the conductivity take the form [6, 7]:

$$\epsilon_n = \sqrt{2eB_o\hbar\left(\frac{v_F^2}{c}\right)\left(n + \frac{1}{2} \pm \frac{1}{2}\right)}; \qquad \sigma_{xy} = \frac{4e^2}{h}\left(\pm n + \frac{1}{2}\right) = \frac{e^2}{h}\nu \tag{42}$$

We measured the integer QHE for our samples by varying the gate voltage at a magnetic field B_o of 8 Tesla, as shown in Fig. 3. The neutrality point is located at -4 V and several Hall plateaus are clearly seen for the Hall resistance R_{xy} for both types of carrier. The longitudinal resistance R_{xx} shows peaks, as expected for the transitions between adjacent plateaus [12], and close to the neutrality point we also observed a sharp Dirac peak, showing the good quality of our graphene sample.

We now consider the transport dependence on the top gate voltage. As can be seen in Fig. 4, in spite of applying very large electric fields in the top-gate, the output is almost independent of the top-gate voltage. It is easy to attribute this behaviour to Klein tunneling, which makes the barrier almost transparent for electrons arriving with a small angle at the top-gate regardless of the gate voltage. In future experiments, it would be interesting to check if at different angles significant differences appear [10]. Also, measuring the conductance phase shift for low magnetic fields could provide additional evidence for the Klein tunneling of relativistic fermions through a potential barrier, as has been recently reported by Young and Kim [13].

Acknowledgements This paper arose as an amplified version of the talk given by one of us (JMC) July 16th, 2010. On that date, people from all over the world got together to congratulate M. Gadella, not because he was 60, but rather his life entirely devoted to physics and his friends. It is extremely hard to find a man like him today: half-monk and half-soldier, in his own words, but truly a friend, to whom many of us will be indebted forever as a noble and singular human being. The authors would also like to thank M. Amado and D. López-Romero for invaluable help in the sample preparation as well as access to CT-ISOM in Madrid. This work has been supported by grants FIS2009-07880 and JCyL SA049A10-2.

References

1. Wallace, P.R.: The band theory of graphite. Phys. Rev. **71**, 622–634 (1947)
2. Semenoff, G.W.: Condensed-matter simulation of a three-dimensional anomaly. Phys. Rev. Lett. **53**, 2449–2452 (1984)
3. Novoselov, K.S., Geim, A.K., et al.: Electric field effects in atomically thin carbon films. Science **306**, 666 (2004)
4. Novoselov, K.S., Geim, A.K., et al.: Two-dimensional gas of massless Dirac fermions in graphene. Nature **438**, 197 (2005)
5. Tan, Y.-W., Störmer, H.L., Kim, P.: Experimental observation of the quantum hall effect and berry phases in graphene. Nature **438**, 201 (2005)
6. Katsnelson, M.: Graphene: carbon in two dimensions. Mater. Today **10**, 20–27 (2007)
7. Castro Neto, A.H., Guinea, F., Peres, N.M.R., Novoselov, K.S., Geim, A.K.: The electronic properties of graphene. Rev. Mod. Phys. **81**, 109–162 (2009)
8. Dombey, N., Calogeracos, A.: Seventy years of the Klein paradox. Phys. Rep. **315**, 41–58 (1999)
9. Thomson, M.J., McKellar, B.H.J.: The solution of the Dirac equation for a high square barrier. Am. J. Phys. **59**, 340–346 (1991)
10. Katsnelson, M., Novoselov, K.S., Geim, A.K.: Chiral tunneling and the Klein paradox in graphene. Nat. Phys. **2**, 620 (2006)
11. Williams, J.R., DiCarlo, L., Marcus, C.M.: Quantum hall effect in a gate-controlled p–n junction of graphene. Science **317**, 638 (2007)
12. Amado, M., Díez, E., López-Romero, D., Caridad, J.M., Dionigi, F., Bellani, V., Maude, D.K.: Plateau insulator transition in graphene. New J. Phys. **12**, 053004 (2010)
13. Young, A.F., Kim, P.: Quantum interference and Klein tunneling in graphene heterojunctions. Nat. Phys. **5**, 222 (2009)